

# STAP-2 Protein Expression in B16F10 Melanoma Cells Positively Regulates Protein Levels of Tyrosinase, Which Determines Organs to Infiltrate in the Body\*

Received for publication, April 15, 2015, and in revised form, May 20, 2015. Published, JBC Papers in Press, May 28, 2015, DOI 10.1074/jbc.M115.658575

Yuichi Sekine<sup>‡</sup>, Sumihito Togi<sup>‡</sup>, Ryuta Muromoto<sup>‡</sup>, Shigeyuki Kon<sup>‡</sup>, Yuichi Kitai<sup>‡</sup>, Akihiko Yoshimura<sup>§</sup>, Kenji Oritani<sup>¶</sup>, and Tadashi Matsuda<sup>‡1</sup>

From the <sup>‡</sup>Department of Immunology, Graduate School of Pharmaceutical Sciences, Hokkaido University, Kita-12 Nishi-6, Kita-Ku, Sapporo, 060-0812, Japan, the <sup>§</sup>Department of Microbiology and Immunology, Keio University School of Medicine, Shinjuku-Ku, Tokyo 160-8582, Japan, the <sup>¶</sup>Department of Hematology and Oncology, Graduate School of Medicine, Osaka University, 2-2 Yamada-oka, Suita, Osaka 565-0871, Japan

**Background:** STAP-2 plays important roles in cell migratory functions.

**Results:** STAP-2 influences the metastatic phenotype of B16 melanoma.

**Conclusion:** STAP-2 regulates B16 melanoma characteristics by modifying tyrosinase content.

**Significance:** This study identifies novel functions of STAP-2 in melanoma metastasis.

Melanoma is the most serious type of skin cancer, with a highly metastatic phenotype. In this report, we show that signal transducing adaptor protein 2 (STAP-2) is involved in cell migration, proliferation, and melanogenesis as well as chemokine receptor expression and tumorigenesis in B16F10 melanoma cells. This was evident in mice injected with STAP-2 shRNA (shSTAP-2)-expressing B16F10 cells, which infiltrated organs in a completely different pattern from the original cells, showing massive colonization in the liver, kidney, and neck but not in the lung. The most important finding was that STAP-2 expression determined tyrosinase protein content. STAP-2 colocalized with tyrosinase in lysosomes and protected tyrosinase from protein degradation. It is noteworthy that B16F10 cells with knocked down tyrosinase showed similar cell characteristics as shSTAP-2 cells. These results indicated that tyrosinase contributed to some cellular events beyond melanogenesis. Taken together, one possibility is that STAP-2 positively regulates the protein levels of tyrosinase, which determines tumor invasion via controlling chemokine receptor expression.

Melanogenesis is a process of production of principal surface pigments in vertebrates and, in humans, plays a major role in photoprotection (1, 2). Melanocytes synthesize melanin within special membrane-limited organelles, called melanosomes, which contain three major pigment enzymes belonging to the tyrosinase-related protein (TRP)<sup>2</sup> family: Tyr, TRP-1, and dop-

achrome tautomerase, also known as TRP-2 (3–5). These three proteins play an essential role in melanogenesis under various control signals (6, 7). For example, the cAMP/PKA pathway up-regulates the expression of the microphthalmia-associated transcription factor (Mitf), which controls the production of melanogenic enzymes (tyrosinase, TRP-1, and TRP-2) at the mRNA level (8–11). Additionally, cAMP activates the ERK pathway, which is also involved in melanin synthesis, at least in part through the regulation of Mitf activation and stability (12–14). Although Mitf-mediated transcriptional activation of pigmentation genes is essential for the control of melanocyte cellular differentiation (12), the up-regulation of *tyrosinase*, *TRP-1*, and *TRP-2* gene transcription in mature melanocytes does not completely explain melanogenesis stimulation by cAMP. Indeed, cAMP signaling can increase the stability of tyrosinase mRNA as well as the enzyme activity of preexisting tyrosinase proteins (15), suggesting that regulation occurs via posttranscriptional events. Furthermore, the process of melanogenesis represents a potential cellular hazard and is confined to special melanosomes in melanocytes, which synthesize pigments and transfer them to recipient cells (2). Melanoma is a type of skin cancer that arises from the aberrant proliferation of melanocytes (16, 17). When melanoma begins to spread, the prognosis deteriorates. Malignant melanocytes tend to exhibit up-regulated melanogenesis and defective melanosomes (2). Therefore, controlling a tyrosinase-dependent mechanism of melanogenesis may be the basis for a potential antimelanoma therapy.

We originally isolated signal transducing adaptor protein 2 (STAP-2) as a c-Fms-interacting protein (18). The amino acid sequence of STAP-2 shows adaptor protein-like structures that carry a pleckstrin homology domain in the N-terminal region and a region distantly related to an Src homology 2 (SH2) in the central region, as well as a proline-rich region and a YXXQ motif in the C-terminal region (18). In our previous work, we found that STAP-2 had the ability to associate with and influence a variety of signaling or transcriptional molecules (18–23).

\* This study was supported in part by the Astellas Foundation for Research on Metabolic Disorders and a grant-in-aid for scientific research from the Ministry of Education, Culture, Sports, Science, and Technology of Japan. The authors declare that they have no conflicts of interest with the contents of this article.

<sup>1</sup> To whom correspondence should be addressed: Dept. of Immunology, Graduate School of Pharmaceutical Sciences, Hokkaido University, Kita-12 Nishi-6, Kita-Ku, Sapporo, 060-0812, Japan. Tel.: 81-11-706-3243; Fax: 81-11-706-4990; E-mail: tmatsuda@pharm.hokudai.ac.jp.

<sup>2</sup> The abbreviations used are: TRP, tyrosinase-related protein; Tyr, tyrosinase; RT-PCR, real-time PCR; ANOVA, analysis of variance; ER, endoplasmic reticulum; OCA, oculocutaneous albinism; PE, phycoerythrin.

For example, STAP-2 can modulate not only the transcriptional activity of STAT3 and STAT5 (18, 19) but also FcεRI and Toll-like receptor-mediated signals (20, 21, 24). Furthermore, thymocytes and peripheral T cells from STAP-2-deficient mice showed enhanced IL-2 or T cell receptor (TCR)-dependent cell growth, elevated integrin-mediated T-cell adhesion, and impaired SDF-1 $\alpha$ -induced T cell migration (19, 22, 23). STAP-2 is now believed to function in various types of cells because it is widely expressed in multiple tissues and cells, such as lymphocytes, macrophages, and hepatocytes (18).

In this study, we found that STAP-2 in murine melanoma B16F10 cells conferred cell migration and cell growth advantage *in vitro* and was able to alter homing sites *in vivo*. We also demonstrated that STAP-2-mediated alteration of cell migration and homing of B16F10 cells was regulated by degradation of tyrosinase. Finally, tyrosinase knockdown in B16F10 cells also showed similar patterns of tumor progression compared with STAP-2 knockdown cells. Therefore, STAP-2 controls the metastatic property of melanoma cells by modulating the lysosomal degradation of tyrosinase.

## Experimental Procedures

**Reagents, Antibodies, and Mice**—Annexin-V-PE was purchased from MBL (Nagoya, Japan). Rhodamine-phalloidin was purchased from Invitrogen. Anti-Myc (9B11) was purchased from Cell Signaling Technology (Beverly, MA). Anti-tyrosinase (M19), anti-TRP1 (A-20), and anti-TRP2 (C-9) antibodies were obtained from Santa Cruz Biotechnology (Santa Cruz, CA). Anti-actin antibodies were from Sigma-Aldrich (St. Louis, MO). Anti-EEA1, anti-Lamp-1, antiGM130, and anti-BiP/GRP78 were obtained from BD Biosciences. Expression vectors for Myc-tagged STAP-2 have been described previously (18). Six- to ten-week-old C57BL/6 background mice were used for all studies. Mice were housed and bred in the Pharmaceutical Sciences Animal Center of Hokkaido University. All animals were maintained under pathogen-free conditions and in compliance with national and institutional guidelines. All protocols were approved by the Hokkaido University Animal Ethics Committee.

**Cell Culture and Establishment of Cell Lines**—The mouse melanoma cell line B16F10 was maintained in DMEM containing 10% FCS. Stable B16F10 transformants were established as described previously (25). Briefly, B16F10 cells ( $1 \times 10^7$ ) were transfected with the pcDNA3 vector (Invitrogen) expressing Myc-tagged human STAP-2 by electroporation, selected in the above medium in the presence of G418 (0.5 mg/ml), and then cloned using the limiting dilution procedure. STAP-2 knockdown B16F10 cell lines (B16F10/shSTAP-2#1, #2 and B16F10/shTyrosinase#1 and #2) were established by transfection of with the pGPU6/GFP/Neo vector (Shanghai GenePharm, Shanghai, China) bearing shRNA targeting STAP-2 (#1, 5-GCGGGCAGGTTCTAAGTATGT-3; #2, 5-GCGGGCAGGTTCTAAGTATGT-3) and shRNA targeting tyrosinase (#1, 5-GCAACTTCATGGTTTCAACT-3; #2, 5-GCCCAAATTGTACAGAGAAGC-3) and then selected with G418 (0.5 mg/ml, Sigma-Aldrich). Similarly, the control shRNA-transfected (nonsilencing, 5-TTCTCCGAACGTGTCACGT-3) B16F10 cell line (B16F10/shControl) was also established.

**Actin Polymerization Assay and Detection of Apoptosis**—Actin polymerization was tested as described previously (26). Briefly, B16F10 cells ( $1 \times 10^6$ ) were cultured in 6-well tissue culture plates for 12 h, and then cells were fixed with 4% paraformaldehyde and treated with 1% Triton X-100 in PBS. Cells were then stained with rhodamine-conjugated phalloidin (Invitrogen) for 30 min. Apoptosis was measured by cytofluorometric analysis. B16F10 cells ( $1 \times 10^6$ ) were cultured in a 6-well plate without or with 10% FCS for 36 h. Then cells were staining with Annexin-V-PE (MBL) according to the instructions of the manufacturer. F-actin content or apoptosis was measured using a FACSCalibur<sup>TM</sup> cytometer (BD Biosciences) and analyzed further using Cell Quest software.

**RT-PCR, and Quantitative Real-time PCR**—RT-PCR analysis was performed using the RT-PCR high-Plus kit (Toyobo). The primers used for RT-PCR were as follows: Tyrp1-5', GTGCT-TGGAGGTCCGTGTAT; Tyrp1-3', CAAAGACCGCATCA-GTGAAA; Tyrp2-5', TACCATCTGTTGTGGCTGGA; Tyrp2-3', CAAGCTGTGCGACACAATCT; Tyr-5', CCTCC-TGGCAGATCATTGT; Tyr-3', GGCAAATCCTTCCAGT-GTGT; CCR1-5', AGGGCCCCGAACCTTACTTT; CCR1-3', TTCCACTGCTTCAGGCTCTT; CCR2-5', ACACCCTG-TTTCGCTGTAGG; CCR2-3' CTGCATGGCCTGGTCTA-AGT; CXCR1-5', TCAGTGGTATCCTGCTGCTG, CXCR1-3', CTGGCGGAAGATAGCAAAAAG; CXCR2-5', ATCTTC-GCTGTGCTCCTTGT; CXCR2-3', AGCCAAGAATCTCC-GTAGCA; CXCR3-5', GCCCTCTACAGCCTCCTCTT, CXCR3-3', AAGGCCCTGCATAGAAGTT; CXCR4-5', TCAGTGGCTGACCTCCTCTT; and CXCR4-3', TTTCAG-CCAGCAGTTTCCTT. Quantitative real-time PCR analyses of STAP-2 as well as the control G3PDH mRNA transcripts were conducted using an assay-on-demand gene-specific fluorescently labeled TaqMan MGB probe in an ABI Prism 7000 sequence detection system (Applied Biosystems).

**Wound Healing Assay**—A wound healing assay was performed as described previously (27). B16F10 cells were cultured in 6-well tissue culture plates as a confluent monolayer, an artificial wound was created by scraping with a yellow pipette tip, and cells migrating into open space were monitored microscopically. Photographs were taken immediately and at various intervals.

**Measurement of Melanin Content**—Melanin content was measured using a modification of a method reported previously (28). B16F10 cells ( $1 \times 10^6$ ) were cultured in 6-well plate for 2 days, collected, and washed twice with PBS. The precipitated cells were resuspended in 200  $\mu$ l of distilled water, and 1 ml of ethanol:ether = 1:1 (v/v) was added to remove opaque substances other than melanin. This mixture was stored at room temperature for 15 min. After further centrifugation, the precipitate was solubilized by treatment with 1 ml of 1 N NaOH, 10% dimethyl sulfoxide at 80 °C for 30 min. The melanin content was measured absorbance at 470–595 nm and expressed as a percent of control.

**In Vivo Tumor Study**—B16F10 cells ( $1 \times 10^5$ ) suspended in PBS were injected intravenously into the tail veins of C57BL/6 mice. Two weeks after intravenous injection, mice were killed, and the lungs were extirpated. Photographs of the lungs were taken immediately, and the black spherical B16F10 colonies

## STAP-2 Modulates B16 Melanoma Metastasis

were counted. To evaluate the length of survival in the tumor-bearing mouse models, mice were injected intravenously with B16 F10 cells ( $1 \times 10^5$ ), and then we monitored their survival.

**Immunoblotting**—Western blotting assays were performed as described previously (19). Briefly, cells were harvested and lysed in lysis buffer (50 mM Tris-HCl (pH 7.4), 0.15 M NaCl, containing 1% Nonidet P-40, 1 mM sodium orthovanadate, and 1 mM phenylmethylsulfonyl fluoride), and then cell lysates were resolved on SDS-PAGE and transferred to a PVDF transfer membrane (PerkinElmer Life Sciences). The filters were then immunoblotted with each antibody. Immunoreactive proteins were visualized using an enhanced chemiluminescence detection system (Millipore).

**Indirect Immunofluorescence Confocal Microscopy**—Parental B16F10 cells were maintained in DMEM containing 10% FCS transfected with Myc-tagged STAP-2 by Lipofectamine 2000. Thirty-six hours after transfection, cells were fixed with a solution containing 4% paraformaldehyde and reacted with respective antibodies. The cells were then reacted with FITC-conjugated anti-goat IgG, rhodamine-conjugated anti-rabbit IgG (Santa Cruz Biotechnology) and Alexa Fluor 647-conjugated anti-mouse IgG antibodies (Invitrogen) and observed under a confocal laser fluorescence microscope. DNA was visualized by DAPI (Wako Chemicals, Osaka, Japan) staining. Images were obtained by using an Olympus Fluoview FV10i-W microscope with an UPLSAPO  $\times 60$  W/numerical aperture 1.2 objective and  $\times 3$  zoom.

**Statistical Methods**—The significance of differences between group means was determined by Student's *t* test or one-way ANOVA, followed by Tukey's test.

## Results

**Manipulation of STAP-2 Expression in Murine Melanoma B16F10 Cells Alters Cell Shape, Cell Migration, and Survival in Vitro**—We have reported previously that Raw264.7 macrophage cells overexpressing STAP-2 showed impaired migration in response to macrophage colony-stimulating factor (M-CSF) and a diminished wound healing process (27). We also showed that STAP-2 regulated SDF-1 $\alpha$ -induced T cell migration via activation of Vav1/Rac1 signaling (23), suggesting that STAP-2 may be widely involved in cell migratory functions. To evaluate this issue in metastatic processes of malignant cells, we employed a highly metastatic murine melanoma cell line, B16F10, that constitutively expresses STAP-2. We initially established STAP-2 knockdown variants of B16F10 cells using shRNA (shSTAP-2 #1 and #2) in which STAP-2 expression was confirmed using real-time PCR (Fig. 1A). ShSTAP-2 cells displayed morphological changes with a more slender shape of elongated axons (Fig. 1B). In parallel with these shape changes, STAP-2 knockdown significantly reduced the phalloidin and F-actin content (Fig. 1, C and D). We then examined the effect of STAP-2 on the migration of B16F10 transfectants. As shown in Fig. 1, E and F, the reduced expression of STAP-2 resulted in a significantly enhanced migration of B16F10 cells in a wound healing assay. Another change of cell characteristics caused by the reduction of STAP-2 was the sensitivity for apoptosis. In shControl but not shSTAP-2 cells, serum depletion induced a significant change in cell morphology, such as a round shape

and detachment from culture dishes (Fig. 1G). These shapes in shControl cells are typical of apoptosis. Indeed, a much higher proportion of shControl cells became annexin V-positive than shSTAP-2 cells (Fig. 1H).

To confirm the above effects of STAP-2, we stably transfected a STAP-2 expression vector into B16F10 cells. Western blot analysis was used to confirm elevated levels of STAP-2 protein in two clones (STAP-2#1 and #2) (Fig. 2A). As shown in Fig. 2, B and C, overexpression of STAP-2 resulted in a significantly reduced migration of B16F10 cells in a wound healing assay, as predicted from the STAP-2 knockdown experiments. Therefore, modification of STAP-2 expression in B16F10 cells showed significant differences in cell morphology, migration, and cell survival compared with shControl cells.

**Specificity of the Alteration of B16F10 Characteristics by STAP-2 Knockdown**—We examined the effect of ectopic expression of human STAP-2 cDNA (huSTAP-2) in STAP-2 knockdown B16F10 cells (shSTAP-2#2). Human STAP-2 expression in shSTAP-2#2 cells was confirmed using Western blot analysis (Fig. 3A). Serum depletion-induced apoptosis in shSTAP-2#2 cells was completely restored by ectopic expression of human STAP-2 (Fig. 3B). The reduced F-actin content was also restored by human STAP-2 (Fig. 3, C and D). Moreover, the enhanced migration of shSTAP-2#2 cells was prevented by human STAP-2 in a wound healing assay (Fig. 3E). Therefore, STAP-2 specifically alters the migration and survival of B16F10 cells.

**Manipulation of STAP-2 Expression in Murine Melanoma B16F10 Cells Alters Tumor Formation in Vivo**—To investigate the effect of STAP-2 on tumor formation *in vivo*, B16F10 transfectants were injected intravenously into C57/B6 mice. As shown in Fig. 4A, mice injected with shControl cells died within 30 days (mean, 25.6 days). The lethality was slightly reduced in those injected with shSTAP-2 cells (shSTAP-2 #1, 27.5 days; #2, 30.6 days). Mice injected with shControl cells showed a massive colonization in the lung (Fig. 4, B and C), as reported previously for B16F10 cells (29). Of importance, mice injected with shSTAP-2 cells developed little lung colonization but showed massive infiltration in the liver, kidney, and neck (Fig. 4D). The different pattern of infiltration was confirmed using Western blot analysis with an anti-GFP antibody (Fig. 4E) and is summarized in Fig. 4F.

We next tested the effect of STAP-2 overexpression on tumor formation. As shown in Fig. 5A, lethality was enhanced in mice injected with STAP-2-overexpressing B16F10 cells (STAP-2 #1, 26.8 days; #2, 28.7 days *versus* the vector control, 35.5 days). Furthermore, mice injected with STAP-2#1 or #2 cells developed much more lung colonization than those injected with vector control cells (Fig. 5, B and C). Therefore, the levels of STAP-2 protein in B16F10 cells determined the pattern of tumor cell infiltration *in vivo*.

**STAP-2 Controls the Protein Content of Tyrosinase in B16F10 Cells**—During a series of experiments, we found that the production of melanin pigment was reduced in shSTAP-2 cells. The reduced melanin content in shSTAP-2 cells is shown in Fig. 6A. In contrast, STAP-2 overexpression increased the melanin content (Fig. 6B). We therefore examined the expression levels of the TRP family of proteins in these transfectants. A marked

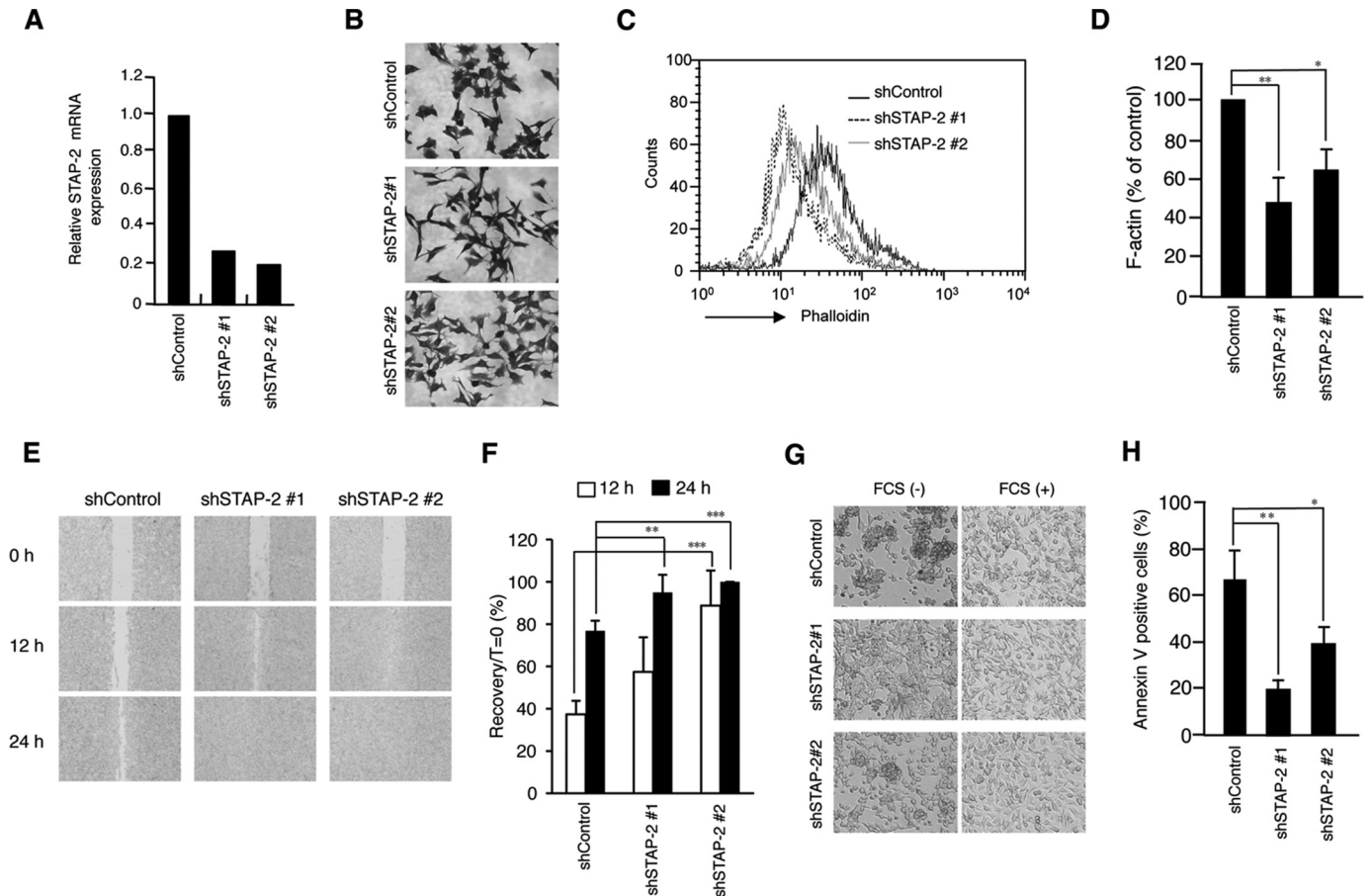


**FIGURE 1. Reduction of STAP-2 in murine melanoma B16F10 cells alters their cell migration and survival.** *A*, shControl and shSTAP-2 #1 and #2 cells were established. Total RNA samples isolated from these cells were quantified by reverse transcription and quantitative real-time PCR analysis. Data represent the levels of STAP-2 mRNA normalized to those of a *G3PDH* internal control and are expressed relative to the value of shControl samples. Data represent the mean of duplicate PCR determinations, which, in general, varied by <10%. Shown is a representative experiment that was repeated at least twice with similar results. *B*, ShControl, shSTAP-2 #1, and shSTAP-2 #2 cells were stained with crystal violet to observe morphological changes by microscopy. *C*, shControl (solid line), shSTAP-2 #1 (dotted line), and shSTAP-2 #2 (gray line) cells ( $1 \times 10^6$ ) were cultured in a 6-well plate for 12 h. The cells were then stained with rhodamine-conjugated phalloidin and analyzed using FACSCalibur and CellQuest software. *D*, the extent of actin polymerization was calculated from three independent experiments. Shown are the mean fluorescence intensity values of F-actin in percent compared with shControl  $\pm$  S.D. \*,  $p < 0.05$ ; \*\*,  $p < 0.01$ ; one-way ANOVA followed by Tukey's test. *E* and *F*, B16F10 cells ( $1 \times 10^6$ ) were cultured in a 6-well plate for 12 h. An artificial wound was created in the B16F10 cell monolayer using a pipette tip. Photographs were taken immediately and again at indicated time periods after creating the wound. Data are representative of four independent experiments (*E*). Cells migrating into the open space beyond the frontiers of the wound edge were quantified. Values are mean  $\pm$  S.D. of four experiments. \*\*,  $p < 0.01$ ; \*\*\*,  $p < 0.005$ ; one-way ANOVA followed by Tukey's test. Similar results were obtained in three independent experiments (*F*). *G* and *H*, B16F10 cells ( $1 \times 10^6$ ) were cultured in a 6-well plate without (-) or with (+) 10% FCS. Photographs were taken 36 h after culture (*G*), and cells cultured without FCS were stained with PE-conjugated Annexin V (*H*). Annexin V-positive apoptotic cells were analyzed using by FACSCalibur and CellQuestPro. Data are the mean  $\pm$  S.D. of three independent experiments. \*,  $p < 0.05$ ; \*\*,  $p < 0.01$ ; one-way ANOVA followed by Tukey's test.

decrease of tyrosinase protein was observed in shSTAP-2 cells (Fig. 6C). STAP-2 knockdown also induced a slight decrease of TRP-1 but not TRP-2 protein. Of importance, mRNA expression of these TRP family proteins was not altered in shSTAP-2 cells. We then examined the protein content of tyrosinase in STAP-2-overexpressing B16F10 cells (STAP-2#1 and #2). As shown in Fig. 6D, a significant increase of tyrosinase protein, but not mRNA, was observed in STAP-2-overexpressing B16F10 cells. These results indicated that the protein levels of STAP-2 were coregulated with those of tyrosinase.

We further tested whether the reduced protein content of tyrosinase in shSTAP-2 cells was specific for STAP-2 knockdown. Human STAP-2-overexpressing shSTAP-2 cells showed almost a complete recovery from the reduction of tyrosinase protein content by shSTAP-2 (Fig. 6E). Similarly, melanin content was also restored in human STAP-2 cDNA-overexpressing shSTAP-2 cells (Fig. 6F). These results indi-

cate that STAP-2 knockdown actually reduces tyrosinase and melanin protein content. Therefore, STAP-2 positively regulates the protein content of tyrosinase at the posttranscriptional level.

*Tyrosinase Regulates Cell Migration, Cell Survival, and Tumor Formation of B16F10 Cells*—To confirm the involvement of tyrosinase in STAP-2-mediated cell migration and tumorigenesis, we established tyrosinase knockdown variants of B16F10 cells using shRNA (shTyr #1 and #2) in which tyrosinase expression was confirmed with Western blot analysis. As shown in Fig. 7A, shTyr#2, but not shTyr#1, could knock down Tyr expression in B16F10 cells. Therefore, we employed Tyr#2 for further experiments. ShTyr#2 cells showed shape changes, a low level of melanin content, escape from apoptosis, reduced F-actin content, and enhanced cell migration (Fig. 7, B–F). It is notable that all changes induced by shTyr#2 were identical to those seen in shSTAP-2 cells.

## STAP-2 Modulates B16 Melanoma Metastasis

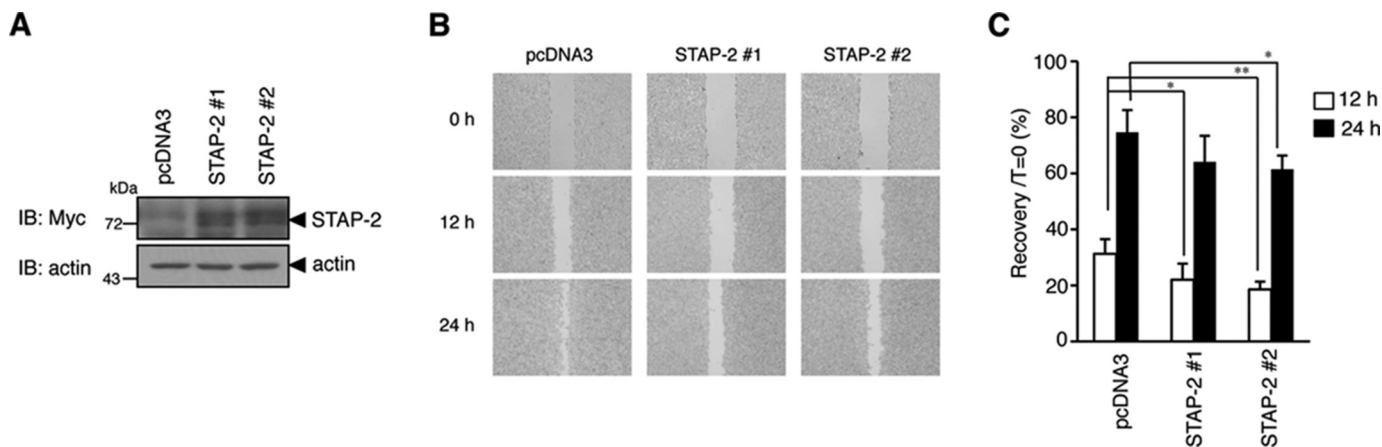


**FIGURE 2. Overexpression of STAP-2 in murine melanoma B16F10 cells alters their cell migration.** *A*, stable B16F10 transfectants overexpressing vector (pcDNA3) or Myc-tagged STAP-2 (STAP-2 #1 and #2) were established. Expression levels of Myc-STAP-2 were analyzed by Western blot using anti-Myc antibody. *B*, immunoblot. *B* and *C*, B16F10 cells were cultured in a 6-well plate. An artificial wound was created in the B16F10 cell monolayer using a pipette tip. Photographs were taken immediately and again at the indicated time periods after creating the wound. Data are representative of five independent experiments (*B*). Cells migrating into the open space beyond the frontiers of the wound edge were quantified. Values are mean  $\pm$  S.D. of five experiments. \*\*,  $p < 0.01$ ; one-way ANOVA followed by Tukey's test (*C*). Similar results were observed in four independent experiments.

We then investigated the effect of tyrosinase on the induction of tumor formation *in vivo*. As shown in Fig. 7*G*, the lethality of mice injected with shTyr#2 cells was not altered compared with shControl cell-injected mice (shTyr#2, 23 days *versus* shControl, 25.3 days). However, mice injected with shTyr#2, but not with shControl cells, formed large tumors in the liver and other sites (Fig. 7, *H* and *I*). Of note, metastatic colonies in the lung were few in shTyr#2 mice, similar as in shSTAP-2 cells (see Fig. 4, *D* and *F*). These results indicated that tyrosinase protein levels influenced cell migration and homing of B16F10 cells *in vivo*. Similar changes in cell characteristics were observed in B16F10 cells with manipulated protein levels of STAP-2 and tyrosinase.

*Both STAP-2 and Tyrosinase Modify the Expression of Chemokine Receptors in B16F10 Cells*—To clarify the mechanisms involved in altered tumor formation in shSTAP-2 or shTyr cells, we examined mRNA expression levels of a series of chemokine receptors in B16F10 transfectants. Control B16F10 cells (shControl#1) expressed CCR1, CCR2, CXCR1, CXCR2, and CXCR4 (Fig. 8, *A* and *B*). However, B16F10 cells transfected with shSTAP-2 or shTyr lost these chemokine receptors but acquired gene expression of CXCR3. The pattern of gene expression of chemokine receptors was identical in shSTAP-2 and shTyr cells.

Therefore, STAP-2 and tyrosinase showed a similar ability to regulate the expression of chemokine receptors.

*STAP-2 Colocalizes with Tyrosinase within Lysosomes and Protects Tyrosinase from Degradation in B16F10 Cells*—To characterize the nature of the functional interactions between STAP-2 and tyrosinase, we attempted to determine where this interaction occurs in B16F10 cells. We transfected Myc-tagged STAP-2 into parental B16F10 cells. In STAP-2-transfected B16F10 cells, STAP-2 colocalized with endogenous tyrosinase in the cytoplasm cell (Fig. 8*C*). As shown in Fig. 8*D*, *first row*, EEA1, an early endosome marker, and GM130, a Golgi marker, did not colocalize with either STAP-2 or tyrosinase. However, both STAP-2 and tyrosinase colocalized with LAMP-1, a lysosome marker, and BiP/GRP78, an endoplasmic reticulum (ER)

marker (Fig. 8*D*, *second through fifth rows*). These images were analyzed for colocalization of STAP-2 and Tyrosinase using the scatterplot of each color pixel intensities. Statistical analysis implied that both STAP-2 and tyrosinase strongly localized in the lysosome and weakly in the ER but not in early endosomes and the Golgi body (data not shown). Notably, both STAP-2 and tyrosinase strongly colocalized with LAMP-1, suggesting that both proteins interacted within the lysosome organelle of B16F10 cells.

We then attempted to examine the coimmunoprecipitation of tyrosinase with STAP-2. However, we could not detect a direct interaction between STAP-2 and tyrosinase in B16F10 cells (data not shown), although both proteins were expressed.

We further tested how tyrosinase content was regulated by STAP-2 in B16F10 cells. To this end, we treated shSTAP-2 cells with inhibitors of proteasomal or lysosomal protein degradation. As shown in Fig. 8*E*, treatment of cells with a proteasome inhibitor, MG132, did not restore tyrosinase content in shSTAP-2 cells. However, treatment of cells with NH<sub>4</sub>Cl, which neutralizes the lysosomal pH and decreases lysosomal protease activities, resulted in a marked recovery of tyrosinase content in shSTAP-2 cells. These data indicated that STAP-2 conferred protein stability of tyrosinase by regulating the lysosomal pathways in B16F10 cells.

## Discussion

We uncovered a novel function of STAP-2 in B16F10 melanoma cells. Manipulation of STAP-2 expression in B16F10 cells resulted in an alteration of tumor cell colonization in cell-injected mice as well as in cell shape, migration and proliferation, melanin production, and chemokine receptor expression. Of importance is that STAP-2 was able to protect tyrosinase from lysosomal degradation. Because B16F10 cells with knocked down tyrosinase showed similar cell characteristics as shSTAP-2 cells, one possibility could be that STAP-2 positively regulates protein levels of tyrosinase, which determines tumor invasion via controlling chemokine receptor expression.

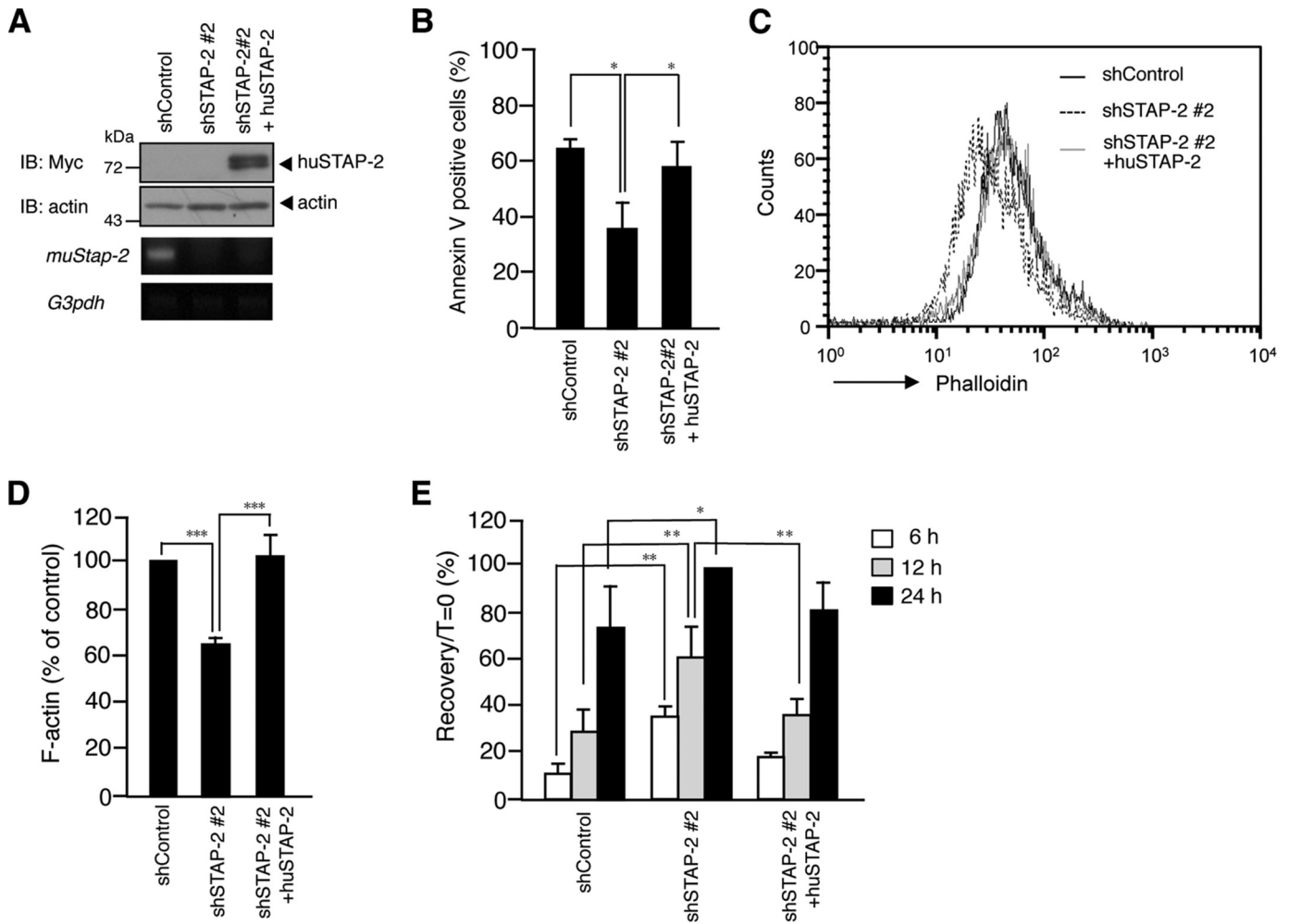


**FIGURE 3. Specificity of the alteration of B16F10 characters by STAP-2 expression levels.** A, a stable shSTAP-2 #2 transfectant expressing human STAP-2 (shSTAP-2 #2 + huSTAP-2) was established. The expression level of human STAP-2 in shSTAP-2 #2 was analyzed by Western blot using anti-Myc and anti-actin antibody. Knockdown of murine STAP-2 was also monitored by RT-PCR with the primers of murine STAP-2 and G3PDH. *B*, immunoblot. *B*, B16F10 cells ( $1 \times 10^6$ ) were cultured in a 6-well plate without FCS for 36 h. The cells were stained with PE-conjugated Annexin V, and apoptotic cells were analyzed using by FACSCalibur and CellQuestPro. Data are the mean  $\pm$  S.D. of three independent experiments. \*,  $p < 0.05$ ; one-way ANOVA followed by Tukey's test. *C*, shControl (solid line), shSTAP-2 #2 (dotted line), and shSTAP-2 #2 + huSTAP-2 (gray line) cells ( $1 \times 10^6$ ) were cultured in a 6-well plate for 12 h, stained with rhodamine-conjugated phalloidin, and monitored by FACSCalibur. *D*, the extent of actin polymerization was calculated from three independent experiments. Shown are the mean fluorescence intensity values of F-actin in percent compared with shControl  $\pm$  S.D. \*\*\*,  $p < 0.005$ , one-way ANOVA followed by Tukey's test. *E*, the indicated cells ( $1 \times 10^5$ ) were cultured in a 6-well plate for 12 h, and an artificial wound was created. Cells migrating into the open space beyond the frontiers of the wound edge were quantified at indicated periods. Values represent the mean  $\pm$  S.D. of triplicate experiments. \*,  $p < 0.05$ ; \*\*,  $p < 0.01$ , one-way ANOVA followed by Tukey's test. Similar results were obtained in three independent experiments.

Melanoma is a malignancy of pigment-producing melanocytes and progresses quickly to undergo tumorigenic evolution. Although available treatments of melanoma include surgery, chemotherapy, immunotherapy, and radiation, only few patients diagnosed with distant metastasis survive for 5 years, indicating the need for new therapeutic approaches. Approximately 50–70% of melanoma cases have a mutation in exon 15 of *BRAF* (30), and recent clinical trials have suggested that inhibition of the BRAF-MAP kinase pathway is expected to prolong progression-free survival and overall survival (31, 32). However, melanoma is still unique in its high melanogenesis capacity and metastasis.

Tyrosinase, which is encoded at the albino locus, is the critical and rate-limiting enzyme required for melanogenesis, catalyzing the initial reaction of tyrosine hydroxylation (33). Mutations in a tyrosinase gene cause an inherited hypopigmentary disease in humans known as oculocutaneous albinism (OCA),

characterized by the reduced or absent pigmentation of the hair, skin, and eyes (34–36). In contrast to mutations in tyrosinase, mutations in the *TYRP1* or *DCT* gene have been shown to affect the quality of melanin synthesized rather than the quantity (4, 37). In humans, mutations in *tyrosinase* result in the most severe form of OCA (OCA1), whereas mutations in *TYRP1* cause a less severe phenotype of the disease (OCA3) (38, 39). Our results clearly indicate that STAP-2 protects tyrosinase protein from degradation in a dose-dependent manner. Indeed, knockdown of STAP-2 reduced tyrosinase content, and B16F10 cells overexpressing STAP-2 showed a high tyrosinase content.

Besides melanogenesis, tyrosinase has cell migration and survival regulatory functions. The B16F10 cell line, originally selected on the basis of a high lung colonization capacity, was established from a spontaneously occurring melanoma in C57BL/6 mice (29). A tyrosinase inhibitor, ascorbic acid, has been shown to inhibit tyrosinase activity and melanin forma-

## STAP-2 Modulates B16 Melanoma Metastasis

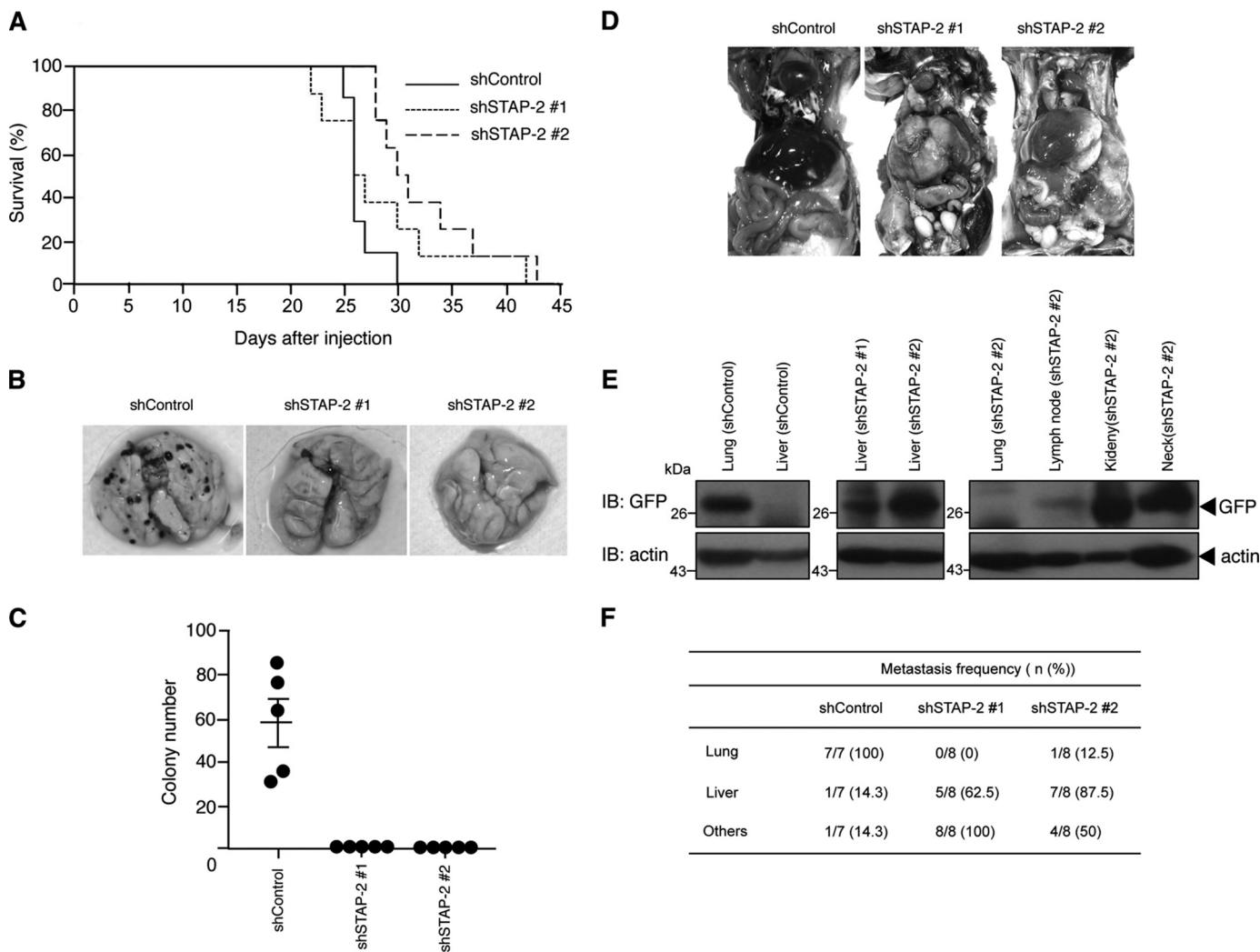


**FIGURE 4. Reduction of STAP-2 in murine melanoma B16F10 cells alters their tumor formation.** *A*, shControl ( $n = 7$ ), shSTAP-2 #1 ( $n = 8$ ), and #2 ( $n = 8$ ) cells ( $1 \times 10^5$ ) were injected intravenously into mice. For  $\sim 45$  days after injection, mouse survival was monitored daily. *B*, shControl, shSTAP-2 #1 and #2 cells ( $1 \times 10^5$ ) were injected intravenously into mice. Two weeks postinjection, the mice were sacrificed, and the lungs were photographed. The photographs show infiltrated cells in melanoma-bearing mice (*C*). B16F10 colonies of the lung were counted. Each circle represents one mouse, and horizontal bars represent the mean.  $n = 5$ ;  $t$ -value for shControl versus shSTAP-2 #1 and #2,  $p < 0.005$ , one-way ANOVA followed by Tukey's test. *D*, the photographs show dead mice in each group. *E*, B16F10-bearing mouse tissues were lysed and immunoblotted (IB) with anti-GFP and anti-actin antibody. *F*, metastasis frequency of B16F10 cells in mouse tissues. Similar results were observed in three independent experiments.

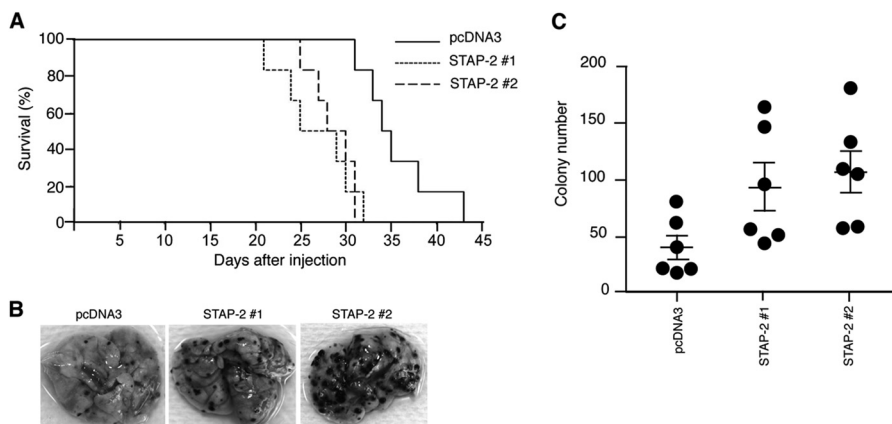


**FIGURE 5. Overexpression of STAP-2 in murine melanoma B16F10 cells alters their tumor formation.** *A*, B16F10/pcDNA3, STAP-2 #1, and #2 cells ( $1 \times 10^5$ ) were injected intraperitoneally into mice. *B* and *C*, for  $\sim 45$  days after injection, mouse survival was monitored daily. B16F10/pcDNA3, STAP-2 #1, and #2 cells ( $1 \times 10^5$ ) were injected intravenously into mice. Two weeks postinjection, the mice were sacrificed, and the lungs were photographed. The photographs show infiltrated cells in melanoma-bearing mice (*B*). B16F10 colonies of the lung were counted. Each circle represents one mouse, and horizontal bars represent the mean.  $n = 6$ ;  $t$ -value for pcDNA3 versus STAP-2 #1,  $p = 0.1124$ ; pcDNA3 versus STAP-2 #2,  $p < 0.05$ ; one-way ANOVA followed by Tukey's test (*C*). Similar results were observed in two independent experiments.

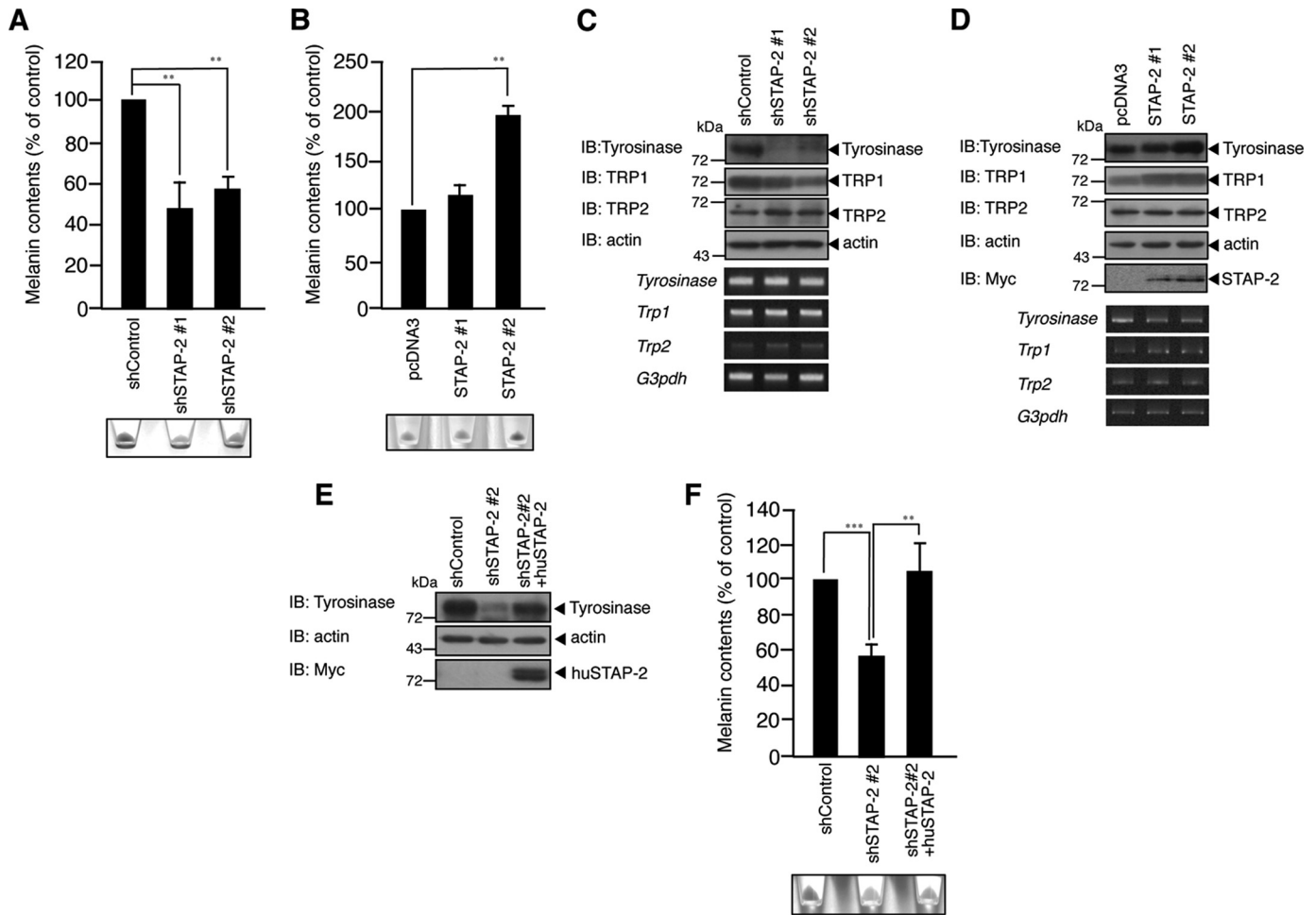


**FIGURE 6. STAP-2 controls the protein content of tyrosinase in B16F10 cells.** *A* and *B*, shControl, shSTAP-2 #1 and #2 cells ( $1 \times 10^6$ ) (*A*) or B16F10/pcDNA3, STAP-2 #1, and #2 cells ( $1 \times 10^6$ ) (*B*) were cultured in a 6-well plate for 2 days. The cells were harvested, the cell pellet was photographed, and the melanin contents were measured as described under "Experimental Procedures." Data are the mean  $\pm$  S.D. of three independent experiments. \*\*,  $p < 0.01$ ; one-way ANOVA followed by Tukey's test. *C* and *D*, shControl, shSTAP-2 #1 and #2 cells ( $1 \times 10^6$ ) (*C*) or B16F10/pcDNA3, STAP-2 #1, and #2 cells ( $1 \times 10^6$ ) (*D*) were lysed and immunoblotted (IB) with anti-tyrosinase, anti-TRP1, anti-TRP2, and anti-actin antibody. Total RNAs were extracted and analyzed for the mRNA expression of tyrosinase, TRP1, TRP2, and G3PDH by RT-PCR. *E*, shControl, shSTAP-2 #2 and shSTAP-2 #2 + huSTAP-2 cells ( $1 \times 10^6$ ) were lysed and immunoblotted with anti-tyrosinase, anti-actin, and anti-Myc antibody. *F*, shControl, shSTAP-2 #2 and shSTAP-2 #2 + huSTAP-2 cells ( $1 \times 10^6$ ) were cultured in a 6-well plate for 2 days. The cells were harvested, the cell pellet was photographed, and the melanin content was measured. Data are the mean  $\pm$  S.D. of three independent experiments. \*\*,  $p < 0.01$ ; \*\*\*,  $p < 0.005$ , one-way ANOVA followed by Tukey's test.

tion in B16 cells (40). A report has shown that ascorbic acid induces the apoptosis of B16 cells via a caspase-8-independent manner *in vitro* (41). These reports suggest an importance of tyrosinase on the melanogenesis and survival of B16 cells. However, no direct evidence of tyrosinase on B16 cell migration and homing *in vivo* has been demonstrated. Importantly, the reduction of protein expression of either STAP-2 or tyrosinase could alter the colonization pattern of B16F10 cells from lung to other tissues, such as liver. Therefore, tyrosinase, whose protein levels are in part regulated by STAP-2, is likely to play crucial roles in melanoma. Additionally, our results suggest possible mechanisms for altered colonization. A number of investigators have reported that melanoma cells express several chemokine receptors, including CCR7, CCR10, and CXCR4. Expression of CCR7 and CCR10 is related to rapid progression and a poorer prognosis (42). B16 melanoma cells overexpressing CCR7 show massive infiltration into draining lymph nodes (43). Additionally, overexpression of CXCR4 in B16 cells is associated with increased metastasis to the lungs (44). Furthermore, a reduced

expression of CXCR3 in B16 cells decreased metastasis to the lymph nodes (45). In this study, protein levels of STAP-2 or tyrosinase significantly affected chemokine receptor expression on B16F10 cells. In particular, CXCR4 expression was decreased significantly and CXCR3 expression was increased when STAP-2 or tyrosinase mRNA was knocked down. Importantly, CXCR3 ligands are known as an interferon-inducible CXC chemokines, such as CXCL9, CXCL10, and CXCL11, and play a critical role in orchestrating type 1 helper cell-mediated immunity by recruiting CXCR3-expressing mononuclear cells (46). CXCR3 ligands are potent inhibitors of angiogenesis and have been shown to be produced by hepatocytes and sinusoidal endothelial cells in the liver (47, 48). Furthermore, CXCR3 has been shown to be important for the recruitment of regulatory T cells into the liver, which might limit inflammatory hepatic injury (49, 50). CXCR3-deficient mice have exhibited pronounced liver fibrosis and exacerbated liver damage after Concanavalin A administration (50). Moreover, CXCL9 administration attenuated angiogenesis and liver fibrosis in mice (51).

## STAP-2 Modulates B16 Melanoma Metastasis

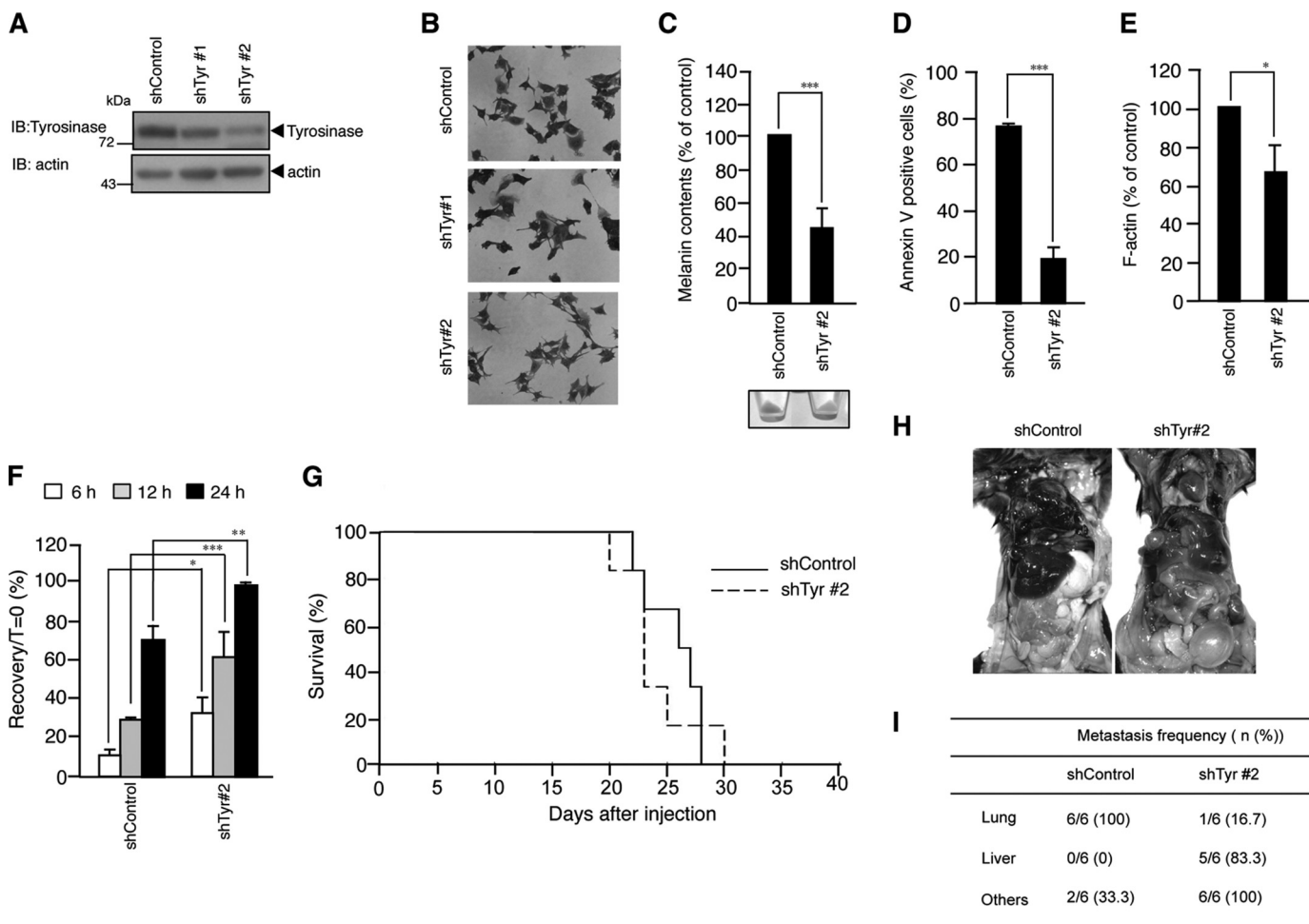


**FIGURE 7. Tyrosinase regulates cell migration, cell survival, and tumor formation of B16F10 cells.** *A*, stable B16F10 transfectants expressing tyrosinase shRNA (#1 and #2) were established. Expression levels of tyrosinase were analyzed by Western blot using anti-tyrosinase and anti-actin antibody. *B*, shControl and shTyrosinase (Tyr) #1 and #2 cells were stained with crystal violet to observe morphological changes by microscopy. *C*, shControl and shTyr #2 cells ( $1 \times 10^6$ ) were cultured in a 6-well plate for 2 days. The cells were harvested, the cell pellet was photographed, and the melanin content was measured. Data are the mean  $\pm$  S.D. of three independent experiments. \*\*\*,  $p < 0.005$ ; Student's *t* test. *D*, shControl and shTyr #2 cells ( $1 \times 10^6$ ) were cultured in a 6-well plate without FCS for 36 h. The cells were stained with PE-conjugated Annexin V, and apoptotic cells were analyzed using FACSCalibur and CellQuestPro. Data are the mean  $\pm$  S.D. of three independent experiments. \*\*\*,  $p < 0.005$ ; Student's *t* test. *E*, the extent of actin polymerization was calculated from three independent experiments. Shown are the mean fluorescence values  $\pm$  S.D. of F-actin in percent compared with shControl. \*,  $p < 0.05$ ; Student's *t* test. *F*, cells ( $1 \times 10^6$ ) were cultured in a 6-well plate for 12 h, and an artificial wound was created. Cells migrating into the open space beyond the frontiers of the wound edge were quantified at the indicated periods. Values represent the mean  $\pm$  S.D. of triplicate experiments. \*,  $p < 0.05$ ; \*\*,  $p < 0.01$ ; \*\*\*,  $p < 0.005$ ; one-way ANOVA followed by Tukey's test. Similar results were obtained in three independent experiments. *G*, shControl and shTyr #2 cells ( $1 \times 10^5$ ) were injected intravenously and monitored over time for their survival ( $n = 6$ ). *H*, the photographs show dead mice in each group. *I*, metastasis frequency of B16F10 cells in mouse tissues.

The recruitment of CXCR3-positive T cells into the kidney has been demonstrated in human and experimental glomerulonephritis (52, 53). Notably, CXCR3-deficient mice show reduced trafficking of effector T cells into the kidney in nephrotoxic nephritis (54). Furthermore, it has been shown that CXCR3 ligands are up-regulated in renal inflammation (55, 56). These findings indicate that the CXCR3/CXCR3 ligand axis has a role in preferential organ accumulation of CXCR3-expressing cells in the body. Therefore, changes in chemokine receptor expression by STAP-2 or tyrosinase may, in part, determine the colonization patterns of B16F10 cells *in vivo*.

One of the most important findings in this work was that STAP-2 regulates the protein content of tyrosinase at the post-transcriptional level. Tyrosinase is known to localize in the ER and is proteolyzed via ER-associated protein degradation. Tyrosinase is also degraded after its complete maturation in the Golgi. Furthermore, tyrosinase protein content is modulated by

ubiquitin-proteasomal degradation. Additional degradation of tyrosinase occurs in lysosomes. Our localization experiments showed that both STAP-2 and tyrosinase were located in lysosomes as well as in the ER and Golgi. We also found that the reduction of tyrosinase protein in shSTAP-2 cells was clearly restored in the presence of  $\text{NH}_4\text{Cl}$ . Therefore, STAP-2 colocalizes with tyrosinase in the same place where tyrosinase processing occurs in melanocytes. Our immunoprecipitation plus Western blot experiment failed to detect a protein association between STAP-2 and tyrosinase. This suggests that STAP-2 interacts indirectly with tyrosinase. STAP-2 expression might regulate the condition and/or activity of lysosomes. Alternatively, their association is weak, which will require optimizing conditions for cell lysis and immunoprecipitation. Further experiments will clarify this issue.

In summary, this study provides evidence that STAP-2 is significantly involved in melanogenesis and that STAP-2

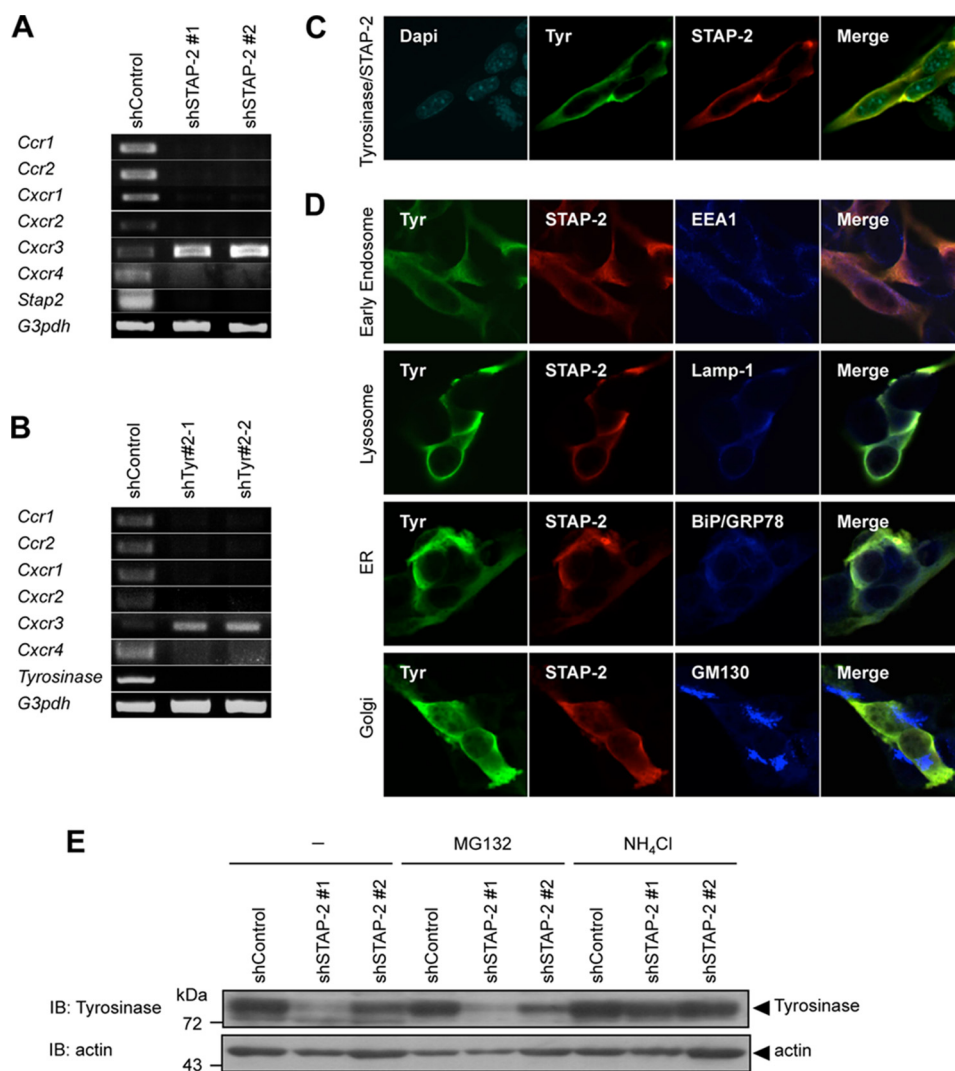


**FIGURE 8. Both STAP-2 and tyrosinase modify the expression of chemokine receptors in B16F10 cells, and STAP-2 colocalizes with tyrosinase within the lysosome and mediates lysosomal degradation of tyrosinase in B16F10 cells.** *A* and *B*, total RNA samples isolated from shControl and shSTAP-2 #1 and #2 cells (*A*) or from ShControl, shTyr #2-1, and #2-2 cells (*B*) were subjected to RT-PCR analysis using CCR1, CCR2, CXCR1, CXCR2, CXCR3, CXCR4, and G3PDH primers. Similar results were observed in three independent experiments. *C*, parental B16F10 cells in a 12-well plate were transfected with Myc-tagged STAP-2 (0.5  $\mu$ g). Thirty-six hours after transfection, the cells were fixed, incubated with anti-tyrosinase and anti-Myc antibody, and visualized with FITC- and rhodamine-conjugated secondary antibody. The same slide was also stained with DAPI to detect nuclei. *D*, parental B16F10 cells in a 12-well plate were transfected with Myc-tagged STAP-2 (0.5  $\mu$ g). Thirty-six hours after transfection, the cells were fixed; incubated with anti-tyrosinase, anti-Myc, and/or anti-EEA1, anti-LAMP-1, anti-BiP/GRP78, and anti-GM130 antibodies; and visualized with FITC-, rhodamine-, and Alexa Fluor 647-conjugated secondary antibody. *E*, shControl and shSTAP-2 #1 and #2 cells ( $1 \times 10^5$ ) in a 12-well plate were treated with MG132 (100  $\mu$ M) or NH<sub>4</sub>Cl (10 mM) for 12 h or left untreated. The cells were lysed and immunoblotted (*IB*) with anti-tyrosinase and anti-actin antibody. Similar results were observed in three independent experiments.

expression plays a crucial role in the metastatic phenotype of melanoma. Therefore, STAP-2 is likely to underlie melanoma progression. Thus, STAP-2 represents a suitable molecular target to establish novel approaches to treat melanoma, and STAP-2 expression has the potential to offer useful insights into the individual characteristics of melanoma in each patient.

**Author Contributions**—Y. S. designed and performed the experiments. S. T., S. K., R. M., and Y. K. analyzed the data. A. Y. distributed the materials. K. O. designed the experiments and wrote the paper, and T. M. designed the experiments, supervised the project, and wrote the paper. All authors analyzed the results and approved the final version of the manuscript.

## References

- Hearing, V. J. (1999) Biochemical control of melanogenesis and melanosomal organization. *J. Investig. Dermatol. Symp. Proc.* **4**, 24–28
- Riley, P. A. (2003) Melanogenesis and melanoma. *Pigment Cell Res.* **16**, 548–552
- Benedito, E., Jiménez-Cervantes, C., Pérez, D., Cubillana, J. D., Solano, F., Jiménez-Cervantes, J., Meyer zum Gottesberge, A. M., Lozano, J. A., and García-Borrón, J. C. (1997) Melanin formation in the inner ear is catalyzed by a new tyrosine hydroxylase kinetically and structurally different from tyrosinase. *Biochim. Biophys. Acta* **1336**, 59–72
- Winder, A., Kobayashi, T., Tsukamoto, K., Urabe, K., Aroca, P., Kamayama, K., and Hearing, V. J. (1994) The tyrosinase gene family: interactions of melanogenic proteins to regulate melanogenesis. *Cell. Mol. Biol. Res.* **40**, 613–626
- Yokoyama, K., Suzuki, H., Yasumoto, K., Tomita, Y., and Shibahara, S. (1994) Molecular cloning and functional analysis of a cDNA coding for human DOPachrome tautomerase/tyrosinase-related protein-2.

- Biochim. Biophys. Acta* **1217**, 317–321
6. Mishima, Y. (1994) Molecular and biological control of melanogenesis through tyrosinase genes and intrinsic and extrinsic regulatory factors. *Pigment Cell Res.* **7**, 376–387
  7. Park, H. Y., and Yaar, M. (2012) *Fitzpatrick's Dermatology in General Medicine*, 8th Ed., pp765–781, McGraw-Hill Medical, New York
  8. Aksan, I., and Goding, C. R. (1998) Targeting the microphthalmia basic helix-loop-helix-leucine zipper transcription factor to a subset of E-box elements *in vitro* and *in vivo*. *Mol. Cell. Biol.* **18**, 6930–6938
  9. Bertolotto, C., Buscà, R., Abbe, P., Bille, K., Aberdam, E., Ortonne, J. P., and Ballotti, R. (1998) Different cis-acting elements are involved in the regulation of TRP1 and TRP2 promoter activities by cyclic AMP: pivotal role of M boxes (GTCATGTGCT) and of microphthalmia. *Mol. Cell. Biol.* **18**, 694–702
  10. Tachibana, M., Takeda, K., Nobukuni, Y., Urabe, K., Long, J. E., Meyers, K. A., Aaronson, S. A., and Miki, T. (1996) Ectopic expression of MITF, a gene for Waardenburg syndrome type 2, converts fibroblasts to cells with melanocyte characteristics. *Nat. Genet.* **14**, 50–54
  11. Bertolotto, C., Abbe, P., Hemesath, T. J., Bille, K., Fisher, D. E., Ortonne, J. P., and Ballotti, R. (1998) Microphthalmia gene product as a signal transducer in cAMP-induced differentiation of melanocytes. *J. Cell Biol.* **142**, 827–835
  12. Buscà, R., Abbe, P., Mantoux, F., Aberdam, E., Peyssonnaud, C., Eychène, A., Ortonne, J. P., and Ballotti, R. (2000) Ras mediates the cAMP-dependent activation of extracellular signal-regulated kinases (ERKs) in melanocytes. *EMBO J.* **19**, 2900–2910
  13. Wong, G., and Pawelek, J. (1975) Melanocyte-stimulating hormone promotes activation of pre-existing tyrosinase molecules in Cloudman S91 melanoma cells. *Nature* **255**, 644–646
  14. Wu, M., Hemesath, T. J., Takemoto, C. M., Horstmann, M. A., Wells, A. G., Price, E. R., Fisher, D. Z., and Fisher, D. E. (2000) *c-Kit* triggers dual phosphorylations, which couple activation and degradation of the essential melanocyte factor Mi. *Genes Dev.* **14**, 301–312
  15. Bertolotto, C., Bille, K., Ortonne, J. P., and Ballotti, R. (1998) In B16 melanoma cells, the inhibition of melanogenesis by TPA results from PKC activation and diminution of microphthalmia binding to the M-box of the tyrosinase promoter. *Oncogene* **16**, 1665–1670
  16. Uong, A., and Zon, L. I. (2010) Melanocytes in development and cancer. *J. Cell. Physiol.* **222**, 38–41
  17. Yamaguchi, Y., and Hearing, V. J. (2014) Melanocytes and their diseases. *Cold Spring Harb. Perspect. Med.* **4**, a017046
  18. Minoguchi, M., Minoguchi, S., Aki, D., Joo, A., Yamamoto, T., Yumioka, T., Matsuda, T., and Yoshimura, A. (2003) STAP-2/BKS, an adaptor/docking protein, modulates STAT3 activation in acute-phase response through its YXXQ motif. *J. Biol. Chem.* **278**, 11182–11189
  19. Sekine, Y., Yamamoto, T., Yumioka, T., Sugiyama, K., Tsuji, S., Oritani, K., Shimoda, K., Minoguchi, M., Yoshimura, A., and Matsuda, T. (2005) Physical and functional interactions between STAP-2/BKS and STAT5. *J. Biol. Chem.* **280**, 8188–8196
  20. Yamamoto, T., Yumioka, T., Sekine, Y., Sato, N., Minoguchi, M., Yoshimura, A., and Matsuda, T. (2003) Regulation of FcεRI-mediated signaling by an adaptor protein STAP-2/BKS in rat basophilic leukemia RBL-2H3 cells. *Biochem. Biophys. Res. Commun.* **306**, 767–773
  21. Sekine, Y., Yumioka, T., Yamamoto, T., Muromoto, R., Imoto, S., Sugiyama, K., Oritani, K., Shimoda, K., Minoguchi, M., Akira, S., Yoshimura, A., and Matsuda, T. (2006) Modulation of TLR4 signaling by a novel adaptor protein signal-transducing adaptor protein-2 in macrophages. *J. Immunol.* **176**, 380–389
  22. Sekine, Y., Tsuji, S., Ikeda, O., Sugiyama, K., Oritani, K., Shimoda, K., Muromoto, R., Ohbayashi, N., Yoshimura, A., and Matsuda, T. (2007) Signal-transducing adaptor protein-2 regulates integrin-mediated T cell adhesion through protein degradation of focal adhesion kinase. *J. Immunol.* **179**, 2397–2407
  23. Sekine, Y., Ikeda, O., Tsuji, S., Yamamoto, C., Muromoto, R., Nanbo, A., Oritani, K., Yoshimura, A., and Matsuda, T. (2009) Signal-transducing adaptor protein-2 regulates stromal cell-derived factor-1  $\alpha$ -induced chemotaxis in T cells. *J. Immunol.* **183**, 7966–7974
  24. Sekine, Y., Nishida, K., Yamasaki, S., Muromoto, R., Kon, S., Kashiwakura, J., Saitoh, K., Togi, S., Yoshimura, A., Oritani, K., and Matsuda, T. (2014) Signal-transducing adaptor protein-2 controls the IgE-mediated, mast cell-mediated anaphylactic responses. *J. Immunol.* **192**, 3488–3495
  25. Sekine, Y., Yamamoto, C., Kakisaka, M., Muromoto, R., Kon, S., Ashitomi, D., Fujita, N., Yoshimura, A., Oritani, K., and Matsuda, T. (2012) Signal-transducing adaptor protein-2 modulates Fas-mediated T cell apoptosis by interacting with caspase-8. *J. Immunol.* **188**, 6194–6204
  26. Wulf, E., DeBoben, A., Bautz, F. A., Faulstich, H., Wieland, T. (1979) Fluorescent phallotoxin, a tool for the visualization of cellular actin. *Proc. Natl. Acad. Sci. U.S.A.* **76**, 4498–4502
  27. Ikeda, O., Sekine, Y., Kakisaka, M., Tsuji, S., Muromoto, R., Ohbayashi, N., Oritani, K., Yoshimura, A., and Matsuda, T. (2007) STAP-2 regulates c-Fms/M-CSF receptor signaling in murine macrophage Raw 264.7 cells. *Biochem. Biophys. Res. Commun.* **358**, 931–937
  28. Ando, H., Funasaka, Y., Oka, M., Ohashi, A., Furumura, M., Matsunaga, J., Matsunaga, N., Hearing, V. J., and Ichihashi, M. (1999) Possible involvement of proteolytic degradation of tyrosinase in the regulatory effect of fatty acids on melanogenesis. *J. Lipid Res.* **40**, 1312–1316
  29. Fidler, I. J. (1975) Biological behavior of malignant melanoma cells correlated to their survival *in vivo*. *Cancer Res.* **35**, 218–224
  30. Davies, H., Bignell, G. R., Cox, C., Stephens, P., Edkins, S., Clegg, S., Teague, J., Woffendin, H., Garnett, M. J., Bottomley, W., Davis, N., Dicks, E., Ewing, R., Floyd, Y., Gray, K., Hall, S., Hawes, R., Hughes, J., Kosmidou, V., Menzies, A., Mould, C., Parker, A., Stevens, C., Watt, S., Hooper, S., Wilson, R., Jayatilake, H., Gusterson, B. A., Cooper, C., Shipley, J., Hargrave, D., Pritchard-Jones, K., Maitland, N., Chenevix-Trench, G., Riggins, G. J., Bigner, D. D., Palmieri, G., Cossu, A., Flanagan, A., Nicholson, A., Ho, J. W., Leung, S. Y., Yuen, S. T., Weber, B. L., Seigler, H. F., Darrow, T. L., Paterson, H., Marais, R., Marshall, C. J., Wooster, R., Stratton, M. R., and Futreal, P. A. (2002) Mutations of the BRAF gene in human cancer. *Nature* **417**, 949–954
  31. Chapman, P. B., Hauschild, A., Robert, C., Haanen, J. B., Ascierto, P., Larkin, J., Dummer, R., Garbe, C., Testori, A., Maio, M., Hogg, D., Lorigan, P., Lebbe, C., Jouary, T., Schadendorf, D., Ribas, A., O'Day, S. J., Sosman, J. A., Kirkwood, J. M., Eggermont, A. M., Dreno, B., Nolop, K., Li, J., Nelson, B., Hou, J., Lee, R. J., Flaherty, K. T., McArthur, G. A., and BRIM-3 Study Group (2011) Improved survival with vemurafenib in melanoma with BRAF V600E mutation. *N. Engl. J. Med.* **364**, 2507–2516
  32. Flaherty, K. T., Robert, C., Hersey, P., Nathan, P., Garbe, C., Milhem, M., Demidov, L. V., Hassel, J. C., Rutkowski, P., Mohr, P., Dummer, R., Trefzer, U., Larkin, J. M., Utikal, J., Dreno, B., Nyakas, M., Middleton, M. R., Becker, J. C., Casey, M., Sherman, L. J., Wu, F. S., Ouellet, D., Martin, A. M., Patel, K., Schadendorf, D., and METRIC Study Group (2012) Improved survival with MEK inhibition in BRAF-mutated melanoma. *N. Engl. J. Med.* **367**, 107–114
  33. Halaban, R., Moellmann, G., Tamura, A., Kwon, B. S., Kuklinska, E., Pomerantz, S. H., and Lerner, A. B. (1988) Tyrosinases of murine melanocytes with mutations at the albino locus. *Proc. Natl. Acad. Sci. U.S.A.* **85**, 7241–7245
  34. Tomita, Y. (1994) The molecular genetics of albinism and piebaldism. *Arch. Dermatol.* **130**, 355–358
  35. Oetting, W. S., and King, R. A. (1999) Molecular basis of albinism: mutations and polymorphisms of pigmentation genes associated with albinism. *Hum. Mutat.* **13**, 99–115
  36. Oetting, W. S. (2000) The tyrosinase gene and oculocutaneous albinism type 1 (OCA1): a model for understanding the molecular biology of melanin formation. *Pigment Cell Res.* **13**, 320–325
  37. Hearing, V. J., Tsukamoto, K., Urabe, K., Kameyama, K., Montague, P. M., and Jackson, I. J. (1992) Functional properties of cloned melanogenic proteins. *Pigment Cell Res.* **5**, 264–270
  38. Boissy, R. E., Zhao, H., Oetting, W. S., Austin, L. M., Wildenberg, S. C., Boissy, Y. L., Zhao, Y., Sturm, R. A., Hearing, V. J., King, R. A., and Nordlund, J. J. (1996) Mutation in and lack of expression of tyrosinase-related protein-1 (TRP-1) in melanocytes from an individual with brown oculocutaneous albinism: a new subtype of albinism classified as "OCA3." *Am. J. Hum. Genet.* **58**, 1145–1156
  39. King, R. A., Pietsch, J., Fryer, J. P., Savage, S., Brott, M. J., Russell-Eggitt, I., Summers, C. G., Oetting, W. S. (2003) Tyrosinase gene mutations in ocu-

- locutaneous albinism 1 (OCA1): definition of the phenotype. *Hum. Genet.* **113**, 502–513
40. Shimada, Y., Tai, H., Tanaka, A., Ikezawa-Suzuki, I., Takagi, K., Yoshida, Y., and Yoshie, H. (2009) Effects of ascorbic acid on gingival melanin pigmentation *in vitro* and *in vivo*. *J. Periodontol.* **80**, 317–323
  41. Kang, J. S., Cho, D., Kim, Y. I., Hahm, E., Yang, Y., Kim, D., Hur, D., Park, H., Bang, S., Hwang, Y. L., and Lee, W. J. (2003) L-ascorbic acid (vitamin C) induces the apoptosis of B16 murine melanoma cells via a caspase-8-independent pathway. *Cancer Immunol. Immunother.* **52**, 693–698
  42. Kühnelt-Leddihn, L., Müller, H., Eisendle, K., Zelger, B., and Weinlich, G. (2012) Overexpression of the chemokine receptors CXCR4, CCR7, CCR9, and CCR10 in human primary cutaneous melanoma: a potential prognostic value for CCR7 and CCR10? *Arch. Dermatol. Res.* **304**, 185–193
  43. Wiley, H. E., Gonzalez, E. B., Maki, W., Wu, M. T., and Hwang, S. T. (2001) Expression of CC chemokine receptor-7 and regional lymph node metastasis of B16 murine melanoma. *J. Natl. Cancer Inst.* **93**, 1638–1643
  44. Murakami, T., Maki, W., Cardones, A. R., Fang, H., Tun Kyi, A., Nestle, F. O., and Hwang, S. T. (2002) Expression of CXC chemokine receptor-4 enhances the pulmonary metastatic potential of murine B16 melanoma cells. *Cancer Res.* **62**, 7328–7334
  45. Kawada, K., Sonoshita, M., Sakashita, H., Takabayashi, A., Yamaoka, Y., Manabe, T., Inaba, K., Minato, N., Oshima, M., and Taketo, M. M. (2004) Pivotal role of CXCR3 in melanoma cell metastasis to lymph nodes. *Cancer Res.* **64**, 4010–4017
  46. Moser, B., and Loetscher, P. (2001) Lymphocyte traffic control by chemokines. *Nat. Immunol.* **2**, 123–128
  47. Belperio, J. A., Keane, M. P., Arenberg, D. A., Addison, C. L., Ehlert, J. E., Burdick, M. D., and Strieter, R. M. (2000) CXC chemokines in angiogenesis. *J. Leukocyte Biol.* **68**, 1–8
  48. Zeremski, M., Petrovic, L. M., and Talal, A. H. (2007) The role of chemokines as inflammatory mediators in chronic hepatitis C virus infection. *J. Viral Hepat.* **14**, 675–687
  49. Santodomingo-Garzon, T., Han, J., Le, T., Yang, Y., and Swain, M. G. (2009) Natural killer T cells regulate the homing of chemokine CXC receptor 3-positive regulatory T cells to the liver in mice. *Hepatology* **49**, 1267–1276
  50. Erhardt, A., Wegscheid, C., Claass, B., Carambia, A., Herkel, J., Mittrücker, H. W., Panzer, U., and Tiegs, G. (2011) CXCR3 deficiency exacerbates liver disease and abrogates tolerance in a mouse model of immune-mediated hepatitis. *J. Immunol.* **186**, 5284–5293
  51. Sahin, H., Borkham-Kamphorst, E., Kuppe, C., Zaldivar, M. M., Grouls, C., Al-samman, M., Nellen, A., Schmitz, P., Heinrichs, D., Berres, M. L., Doletschel, D., Scholten, D., Weiskirchen, R., Moeller, M. J., Kiessling, F., Trautwein, C., and Wasmuth, H. E. (2012) Chemokine Cxcl9 attenuates liver fibrosis-associated angiogenesis in mice. *Hepatology* **55**, 1610–1619
  52. Segerer, S., Banas, B., Wörnle, M., Schmid, H., Cohen, C. D., Kretzler, M., Mack, M., Kiss, E., Nelson, P. J., Schlöndorff, D., and Gröne, H. J. (2004) CXCR3 is involved in tubulointerstitial injury in human glomerulonephritis. *Am. J. Pathol.* **164**, 635–649
  53. Romagnani, P., Beltrame, C., Annunziato, F., Lasagni, L., Luconi, M., Galli, G., Cosmi, L., Maggi, E., Salvadori, M., Pupilli, C., and Serio, M. (1999) Role for interactions between IP-10/Mig and CXCR3 in proliferative glomerulonephritis. *J. Am. Soc. Nephrol.* **10**, 2518–2526
  54. Panzer, U., Steinmetz, O. M., Paust, H. J., Meyer-Schwesinger, C., Peters, A., Turner, J. E., Zahner, G., Heymann, F., Kurts, C., Hopfer, H., Helmchen, U., Haag, F., Schneider, A., and Stahl, R. A. (2007) Chemokine receptor CXCR3 mediates T cell recruitment and tissue injury in nephrotoxic nephritis in mice. *J. Am. Soc. Nephrol.* **18**, 2071–2084
  55. Panzer, U., Steinmetz, O. M., Reinking, R. R., Meyer, T. N., Fehr, S., Schneider, A., Zahner, G., Wolf, G., Helmchen, U., Schaerli, P., Stahl, R. A., and Thaiss, F. (2006) Compartment-specific expression and function of the chemokine IP-10/CXCL10 in a model of renal endothelial microvascular injury. *J. Am. Soc. Nephrol.* **17**, 454–464
  56. Avihingsanon, Y., Phumesin, P., Benjachat, T., Akkasilpa, S., Kittikowit, V., Praditpornsilpa, K., Wongpiyabavorn, J., Eiam-Ong, S., Hemachudha, T., Tungsanga, K., and Hirankarn, N. (2006) Measurement of urinary chemokine and growth factor messenger RNAs: a noninvasive monitoring in lupus nephritis. *Kidney Int.* **69**, 747–753